

Elucidating the Roles of SiO₂ and MnO upon Decarburization During Submerged Arc Welding: A Thermodynamic Study into EH36 Shipbuilding Steel



JIN ZHANG, THERESA COETSEE, HONGBIAO DONG, and CONG WANG

By employing CaF₂-SiO₂ and CaF₂-SiO₂-MnO system fluxes, the roles of SiO₂ and MnO in decarburization behaviors during submerged arc welding of EH36 shipbuilding steel have been quantified and evaluated. All possible reactions associated with C transfer and interfaces at which these reactions occur are systematically discussed. It is concluded that the addition of SiO₂ and MnO exerts synergistic effects on the extent of decarburization due to increased partial pressures of O₂ and SiO gases in the plasma, improved O level in the weld pool, and higher activities of the oxides, such as SiO₂, MnO, and FeO, at the slag-metal interface. The investigation over the macrographic detached slag surfaces shows that the possibility of bubble nucleation is highly influenced by flux formula. The effect of heat input on decarburization is discussed, and the optimal flux compositions expected in the present study are analyzed.

<https://doi.org/10.1007/s11663-020-01869-x>

© The Minerals, Metals & Materials Society and ASM International 2020

I. INTRODUCTION

C is an essential element in the weld metal (WM) for steel grades. It is widely accepted that an increase in C composition enhances steel strength and hardness; however, redundant C may cause a reduction in elongation, toughness, and weldability.^[1] C is also one of the most effective soluble elements to influence acicular ferrite (AF) formation, the level of which must be optimized to reach maximum AF fraction in the WM since the formation of AF tends to be suppressed with excessive C content.^[2-4]

Submerged arc welding (SAW) has been widely used for the joining of thick workpieces due to its inherently high deposition rate and welding efficiency.^[5] During SAW, flux is employed to separate the arc and the weld pool from the atmosphere.^[6] One salient characteristic of SAW is the significant O uptake from the flux (slag),

which will inevitably lead to the decarburization in SAW.^[7-12] Therefore, it is essential to understand the decarburization mechanisms in SAW to ensure a sound weld.

The behaviors of decarburization in SAW have been discussed previously. Mitra *et al.*^[9] reported that C was oxidized *via* the gas-metal interfacial reaction between dissolved C and O in the weld pool; they postulated that CO nucleation was feasible and could be responsible for the bubbles under the slag. Indacochea *et al.*,^[8] on the other hand, emphasized the importance of the net decarburization reactions between SiO₂ in the slag, gases (SiO and O₂) in the plasma, and C in the weld pool; they assumed that CO only tended to nucleate at the plasma-metal interface. Bang *et al.*^[13] performed SAW with different fluxes and found that C loss from the WM generally increased with lower flux basicity.

Generally, flux is the major source of O contamination^[7,14] and plays an important role in decarburization control as a result of the following reasons:

1. In the presence of the welding arc, most oxide components in the flux tend to decompose and release gases (such as O₂ and SiO)^[5,11,15-17] which may react with C in the weld pool at the gas-metal interface.^[8]
2. The level of O dissolved in the weld pool, which largely determines the extent of decarburization, is highly dependent on the oxide decomposition behaviors and slag-metal reactions.^[1,6,11]
3. Reactions between C dissolved in the weld pool and oxides in the molten slag may occur.^[10]

JIN ZHANG is with the School of Metallurgy, Northeastern University, Shenyang 110819, China; THERESA COETSEE is with the Department of Materials Science and Metallurgical Engineering, University of Pretoria, Pretoria, 0002, South Africa; HONGBIAO DONG is with the School of Metallurgy, Northeastern University and also with the Department of Engineering, University of Leicester, Leicester LE1 7RH, UK; CONG WANG is with the School of Metallurgy, Northeastern University and also with the State Key Laboratory of Rolling and Automation, Northeastern University, Shenyang 110819, China. Contact e-mail: wangc@smm.neu.edu.cn

Manuscript submitted March 16, 2020.

Article published online May 26, 2020.

The impact of flux formulas on the WM compositions, including O and metallic elements (such as Si, Mn, Ti, and Cr, *etc.*), has been extensively investigated.^[1,9,11,17-22] However, there are rarely systematic studies done on how flux components influence decarburization behaviors in SAW.

CaF₂, which intrinsically exerts no O potential, plays the role of lowering the melting temperature of the flux.^[11] SiO₂ and MnO are basic components and primary sources of O for flux.^[11] SiO₂, acting as silicate network former in the slag,^[23] is an indispensable ingredient for flux design to ensure slag detachability^[16]; MnO is added in the flux to avoid Mn loss from the weld pool or to micro-alloy the WM with Mn during SAW.^[8,17] The present study is undertaken to elucidate the roles of SiO₂ and MnO in decarburization behaviors during SAW by applying thermodynamic considerations. The impacts of SiO₂ and MnO on C transfer are quantified, and possible decarburization reactions in SAW are thoroughly evaluated. Although the SAW environment is complex due to large density gradient, presence of multiple phases, and high radiative energy from the arc, knowledge of thermodynamics can still be applied to analyze C transfer behaviors by assuming that equilibrium is locally attained.^[8,10,17,18,24]

II. MATERIALS AND EXPERIMENTAL METHODS

Two series of fluxes in CaF₂-SiO₂ and CaF₂-SiO₂-MnO systems, with formulas listed in Table I, were designed to acquire the gradients of flux O potentials. The production and compositional analysis of the fluxes followed the procedures stated in our previous studies.^[16,17]

SAW was performed by bead-on-plate welding method on EH36 shipbuilding steel base metal (BM) of 24 mm thickness. Double-wire welding was applied with heat input of approximately 60 kJ/cm (DC-850 A/

32 V for electrode forward, AC-625 A/36 V for electrode backward, welding speed: 500 mm/min). To determine the WM geometries, the welds were cross-sectioned, polished, and etched by 4 wt pct nital solution.

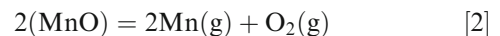
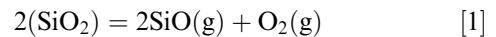
A coupled plasma optical emission spectrometry (ICP-OES) (Perkin Elmer Optima 8300 DV ICP-OES) was employed to analyze metallic element content. LECO analyzers were used to determine C and O contents. Compositions of BM and electrode are shown in Table II.

To exclude the dilution effects of BM and electrode in welding, a commonly defined Δ value, which is widely applied to quantify the compositional contribution from the flux, is introduced.^[10,24,25] A positive Δ value indicates that the flux promotes the gain of C in the WM, whereas a negative Δ value implies that the flux leads to C loss from the WM. The absolute value of Δ means the amount of C transfer. The nominal C composition, which is confirmed from the WM geometry, means the C content considering only the simple mixing of electrode and BM. The calculation methods of nominal composition and Δ value are stated elsewhere.^[8,16] The compositions of O and C in WMs are shown in Table III (subscript 'A': analytical composition, subscript 'N': nominal composition).

III. RESULTS AND DISCUSSION

The major phases and reaction interfaces associated with gas phases in SAW are illustrated in Figure 1. Figure 1(a) shows the schematic illustration of the SAW process. The reaction interfaces in contact with the plasma are plotted in Figure 1(b), and those in contact with the gas bubble are plotted in Figure 1(c). During SAW, the plasma and weld pool are separated from the atmosphere by a layer of molten slag and granular flux;^[5] therefore, the major gas phases in SAW are plasma together with gas bubble (if it exists) under the slag, and CO nucleation barriers disappear when the gas phases contact the weld pool. Generally, the reactions which may influence decarburization behaviors can be divided into three categories: gas-metal, gas-slag, and gas-slag-metal reactions.

The decarburization reactions in the plasma will be discussed first. The presence of the interfaces in Figure 1(b) has been confirmed previously.^[6] At the plasma-slag interface, most oxides, especially SiO₂ and MnO, tend to decompose and release gases *via* Reactions [1] and [2].^[5,11]



Due to decomposition, P_{O_2} in the plasma increases, and the O content of the droplet is promoted to a relatively high level.^[7] Richardson sampled droplets and discovered that there was little exchange of C despite the

Table I. Formulas of Fluxes Employed (Weight Percent)

Fluxes	Flux Systems	Flux Formulas		
		CaF ₂	SiO ₂	MnO
F-1	CaF ₂ -SiO ₂	95	5	0
F-2		90	10	0
F-3		85	15	0
F-4		80	20	0
F-5		70	30	0
F-6	CaF ₂ -SiO ₂ -MnO	60	40	0
F-7		50	40	10
F-8		40	40	20
F-9		30	40	30
F-10		20	40	40
F-11		10	40	50
F-12		0	40	60

Table II. Chemical Compositions of BM and Electrode (Weight Percent)

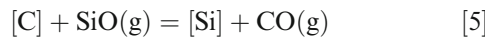
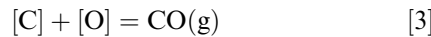
	C	Si	Mn	Ti	Nb	Ni	Cr	O
Base Metal	0.052	0.142	1.540	0.010	0.013	0.075	0.028	0.003
Electrode	0.127	0.049	1.650	0.010	0.004	0.009	0.030	0.003

Table III. Chemical Compositions of O and C in WMs (Weight Percent)

Weld Metals	Fluxes	Compositions of Weld Metals			
		(O) _A	(C) _A	(C) _N	ΔC
WM-1	F-1	0.0090	0.0840	0.0944	- 0.0104
WM-2	F-2	0.0110	0.0810	0.0931	- 0.0121
WM-3	F-3	0.0100	0.0790	0.0891	- 0.0101
WM-4	F-4	0.0110	0.0710	0.0851	- 0.0141
WM-5	F-5	0.0120	0.0670	0.0855	- 0.0185
WM-6	F-6	0.0180	0.0690	0.0913	- 0.0223
WM-7	F-7	0.0360	0.0650	0.0807	- 0.0157
WM-8	F-8	0.0410	0.0540	0.0827	- 0.0287
WM-9	F-9	0.0480	0.0490	0.0847	- 0.0357
WM-10	F-10	0.0610	0.0520	0.0808	- 0.0288
WM-11	F-11	0.0880	0.0530	0.0879	- 0.0349
WM-12	F-12	0.0830	0.0440	0.0805	- 0.0365

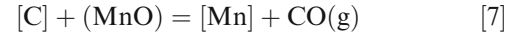
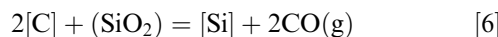
high O level in the droplets.^[26] Mitra *et al.*^[15,20] postulated that an O layer was built up at the droplet–plasma interface, as exhibited in Figure 1(b). This active O layer prevents C from reaching the interface, and thus, decarburization is hindered.

After the droplet is diluted in the weld pool, C is oxidized under the plasma. At the plasma–metal interface, Reactions [3], [4], and [5] are essential for C transfer.



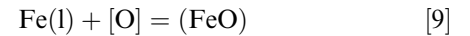
The importance of Reaction [3] on decarburization has been discussed extensively.^[8,9,13] As for Reactions [4] and [5], knowledge of the exact gas composition in the plasma is not known,^[6] therefore, Gibbs free energy change (ΔG) calculation with different partial pressures were performed with results illustrated in Appendix A (Figure A1), from which it is seen that Reactions [4] and [5] play larger roles in decarburization with lower P_{CO} - to - P_{O_2} and P_{CO} -to- P_{SiO} ratios.

At the plasma–slag–metal interface, decarburization *via* Reactions [6], [7], and [8] should be considered.



The possibility of Reactions [6] was postulated by Indacochea *et al.*,^[8] although thermodynamic calculations were not performed. As is seen from Figure A1, even at the highest activity values of SiO_2 and MnO expected in the calculations for Reactions [6] and [7], Reaction [3] and possibly Reaction [4] are more likely occurrences.

It should be noted that FeO is formed from the oxidation of Fe *via* Reaction [9], which generally proceeds forward, at the slag–metal interface^[20]; this was confirmed by our previous studies since FeO was analyzed in the slags of Fe-oxides-free fluxes.^[16,17]



Nonetheless, Reaction [8] appears to be of less importance since the fluxes do not contain any Fe-oxides, and thus, the activity of FeO would be negligible.^[16,17]

As for the decarburization relations in the zone of Figure 1(c), bubble nucleation is important for these reactions to occur due to the tendency of CO release. However, the possibility of bubble nucleation under the slag is unclear, as mentioned above.^[8,9] Therefore, typical macrographic images of the detached slag surfaces with corresponding flux formulas are investigated and exhibited in Figure 2. Typical bubble size was quantified by the linear intercept method.^[27]

For Fluxes F-1 and F-2, the slag surfaces show typical ‘fish scale’ patterns, and no bubble is observed, as illustrated in Figures 2(a) and (b). When the level of SiO_2 is up to 40 wt pct in the binary CaF_2 - SiO_2 flux (Flux F-6), large amount of bubbles appear as the case in Figure 2(f) with average bubble diameter of 1.43 mm. For Fluxes F-7 and F-8, the addition of MnO of 10 and 20 wt pct at the expense of CaF_2 leads to the formation of large bubbles (average typical large bubble diameter of 12.92 mm in Flux F-7 and 18.34 mm in Flux F-8) from an observation in Figures 2(g) and (h). For Flux F-9, large bubbles disappear, and the average bubble diameter is quantified to be 1.55 mm in Figure 2(i). With further MnO addition, the bubble sizes become smaller, as illustrated in Figures 2(j) and (k). However, for CaF_2 -free flux, *viz.* Flux F-12, the bubble disappears, and smooth slag surface is obtained, as shown in Figure 2(l).

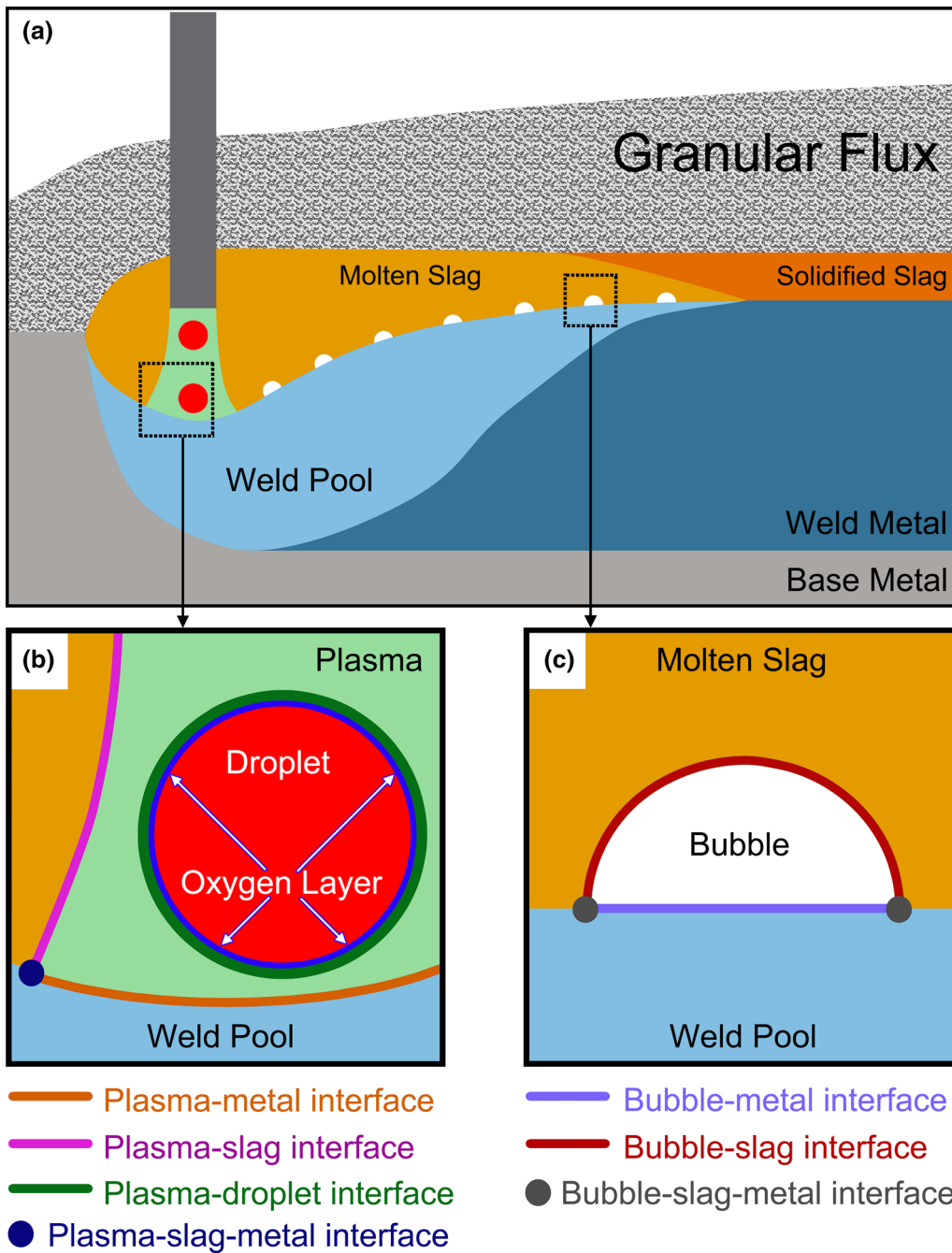


Fig. 1—Major phases and reaction interfaces associated with gas phases in SAW: (a) schematic diagram of SAW, (b) plasma-associated reaction interfaces, (c) bubble-associated reaction interfaces.

Indacochea *et al.*^[8] speculated that bubble nucleation is hindered due to high surface and interfacial tensions of silicates and the weld pool. It seems that Indacochea's assumption is not feasible in the present study as bubbles did appear even if SiO₂-containing fluxes are employed. Based on the observation in Figure 2, the nucleation and release of bubbles are closely related to flux composition, although the mechanisms are not fully understood since the effective temperature of the slag-metal reaction in SAW is as high as 2273 K,^[1,18] and the data of thermophysical properties of the slags at

this temperature remain scarce.^[28] Possible factors that influence nucleation and the release of the bubbles for the present flux systems are as follows:

1. Generally, it is expected that the addition of CaF₂ tends to decrease the surface tension and viscosity of the slag, which would drive the bubble release to a larger extent.^[29,30] This is reflected by the typical larger bubbles illustrated in Figures 2(g) and (h) when CaF₂-rich fluxes of CaF₂-SiO₂-MnO systems are employed.

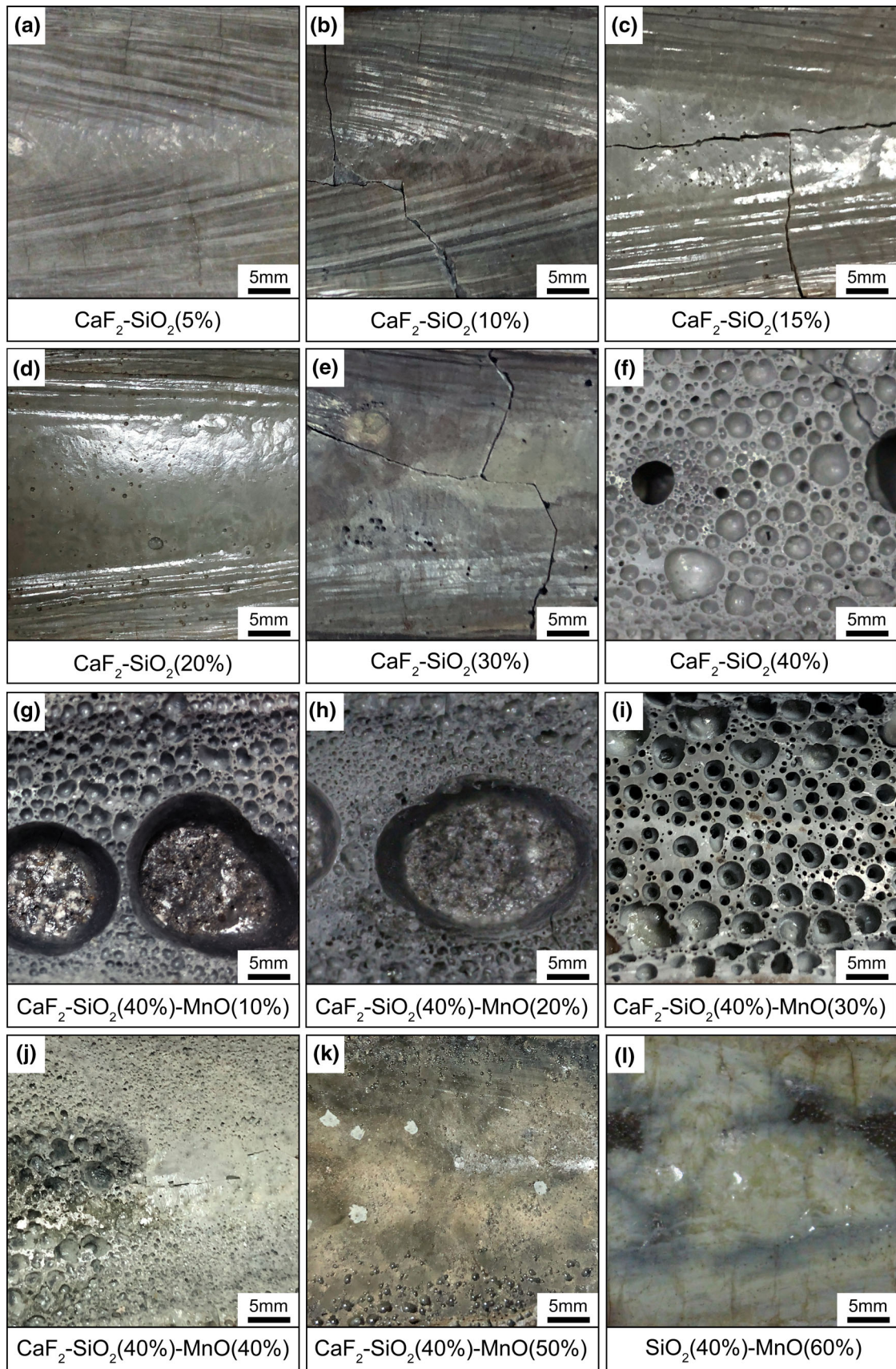


Fig. 2—Macrographic images of the detached slag surfaces with the corresponding flux formulas (weight percent): (a) Flux F-1, (b) Flux F-2, (c) Flux F-3, (d) Flux F-4, (e) Flux F-5, (f) Flux F-6, (g) Flux F-7, (h) Flux F-8, (i) Flux F-9, (j) Flux F-10, (k) Flux F-11, and (l) Flux F-12.

2. It appears that the formation of SiF_4 gas (via Reaction [A1]) is closely related to the bubble nucleation. For $\text{CaF}_2\text{-SiO}_2$ system fluxes, the highest level of SiF_4 formation is expected for Flux F-6 according to the maximum reduction of both CaF_2 and SiO_2 analyzed in our previous study,^[16] which may account for the nucleation of bubbles shown in Figure 2(f). For $\text{CaF}_2\text{-SiO}_2\text{-MnO}$ system fluxes, no bubble is observed when CaF_2 -free flux, viz. Flux F-12 is used, as no formation of SiF_4 gas is expected, as shown in Figure 2(l).

Figure 1(c) illustrates all possible bubble-involved interfaces (if the bubble is nucleated under the slag); the presence of the interfaces in Figure 1(c) is well corroborated by the surface macrographic images illustrated in Figure 2(g) and (h). Possible reactions which may influence C transfer in this zone include the following:

1. Reaction [3] at the bubble-metal interface;
2. Reactions [6], [7], and [8] at the bubble-slag-metal interface.

However, the atmosphere in the bubbles is complex. To perform ΔG calculations and determine the possibility for decarburization reactions in this zone to occur, precise knowledge of gaseous conditions in the bubble is required. If bubbles form due to the entrapment of gases from the plasma, they may likely contain O_2 and SiO , and, under such circumstance, Reactions [4] and [5] should be considered.^[9] It is noted that P_{CO} may likely be less than 0.1 atm due to the low C levels in both the BM and the electrode, which would drive the ΔG values in Figure A1 more negative.

Based on the decarburization mechanisms discussed above, the effects of SiO_2 and MnO in fluxes on C transfer are discussed. For $\text{CaF}_2\text{-SiO}_2$ binary fluxes, variations of ΔC and O in WMs are plotted in Figure 3. It is noted from Figure 3 that C loss from the WM increases from 0.0101 to 0.0223 wt pct, while O content in the WM increases from 0.009 to 0.018 wt pct with higher SiO_2 level (5 to 40 wt pct) in the flux. Increased SiO_2 addition promotes Reactions [1] and [10] to the right side, resulting in the higher extent of SiO_2 decomposition into gases (higher P_{O_2} and P_{SiO}) and O level of the weld pool, which is reflected by the increasing O composition in the WM as shown in Figure 3.^[16] Therefore, C loss from the WM is facilitated as Reactions [3], [4], and [5] are driven to the right side.



Additionally, with the increase of SiO_2 content in the flux, the activity of FeO at the slag-metal interface, which is proportional to the O level in the WM, increases^[8,16]; the decarburization level is, thus, enhanced since Reaction [8] is promoted to the right side. Increased SiO_2 in the flux also drives Reaction [6] to the right side as the activity of SiO_2 at the slag-metal interface is increased.^[16]

As is seen from Figure 4, for ternary $\text{CaF}_2\text{-SiO}_2\text{-MnO}$ fluxes, increased addition of MnO from 10 to 60 wt pct promotes the extent of decarburization from 0.0157 to 0.0365 wt pct. O content in the WM generally increases with higher MnO content due to higher degree of MnO decomposition via Reaction [2] and higher level of O transfer to the weld pool via Reaction [11], as shown in Figure 4.^[17] Thus, it is expected that ΔC value is

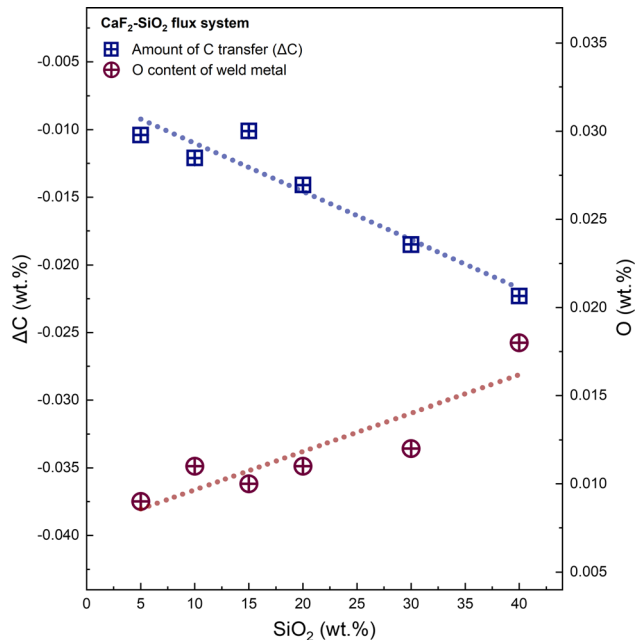


Fig. 3— ΔC and O variations in the WMs as a function of SiO_2 content in $\text{CaF}_2\text{-SiO}_2$ fluxes.

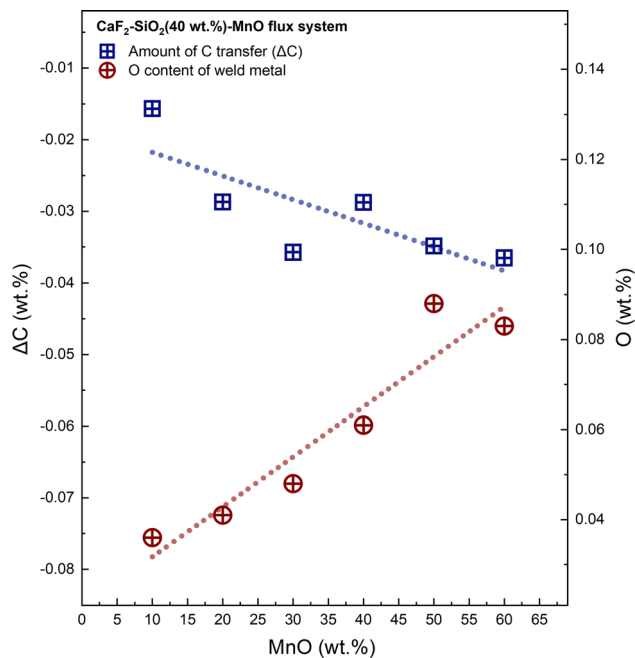
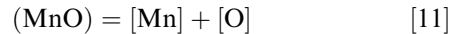


Fig. 4— ΔC and O variations in the WMs as a function of MnO content in $\text{CaF}_2\text{-SiO}_2\text{-MnO}$ fluxes.

decreased as Reactions [3] and [4] are driven to the right side. Also, with the increase of MnO addition, the activities of MnO and FeO (proportional to O level in the WM) at the slag–metal interface are increased,^[17] which leads to higher extent of C loss through Reactions [7] and [8].



It is accepted that a higher extend of oxide decomposition tends to occur with increasing heat input, and both Reactions [1] and [2] are expected to be driven to the right sides, leading to the improvement of P_{O_2} and P_{SiO} in the plasma and O level in the weld pool; therefore, the C loss from the weld pool tends to be promoted as Reactions [3], [4], and [5] are shifted to the right sides.^[7,17,23] According to the screening experiments performed by Chai,^[1] the influence of welding speed on C transfer behaviors is negligible.

Loder *et al.*^[4] reported that the formation of AF is suppressed when C level is higher than 0.65 wt pct. In addition to C, O is the most important element that controls the mechanical properties, especially the toughness of the weld.^[24,31] Ito *et al.*^[32] concluded that the O level in the WM should be controlled in the range from 200 to 500 ppm. Based on the optimal ranges of C and O levels raised by Loder *et al.*^[4] and Ito *et al.*,^[32] Fluxes F-8 and F-9 are expected as the optimal flux compositions in this work (see Table III). For the current SAW condition, the MnO level in CaF₂-SiO₂-MnO system fluxes should be restricted to be less than 30 wt pct to avoid redundant O gaining from the fluxes.

For C-free fluxes, the addition of SiO₂ and MnO would also cause the decarburization in the SAW process for other steel grades, which is confirmed by previous studies.^[8,10,23] However, the C composition in the final WM is contributed from the electrode, BM, and flux (slag).^[10,24,25] To better control the C level and achieve desired mechanical properties, overall consideration of the selection of welding consumables (electrode, BM, and flux) and understanding of chemical decarburization reaction in SAW is necessary. When steels of high C levels are welded, fluxes with higher levels of SiO₂ and MnO and electrodes with lower C levels are recommended to match the BMs.^[10]

IV. CONCLUSIONS

In summary, from a thermodynamic viewpoint, this study offers an in-depth investigation detailing the roles of SiO₂ and MnO in decarburization behaviors during SAW. All possible decarburization reactions with associated interfaces are thoroughly investigated and evaluated. It is concluded that higher additions of SiO₂ and MnO into fluxes exert synergistic effects on the extent of decarburization due to higher partial pressures of the gases (O₂ and SiO) in the plasma, improvement of the O level in the weld pool, and increased activities of the oxides (SiO₂, MnO, and FeO) at the slag–metal interface. The decarburization mechanisms and quantified ΔC values investigated in this study may present viable

options towards flux design and matching strategies of welding consumables in SAW.

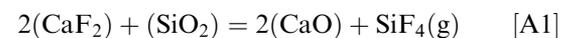
ACKNOWLEDGMENTS

We thank the National Natural Science Foundation of China (Grant Nos. 51622401, 51861130361, 51861145312, and 51850410522), Newton Advanced Fellowship by the Royal Society (Grant No. RP12G0414), Research Fund for Central Universities (Grant Nos. N172502004, N2025025), Xingliao Talents Program (XLYC1807024 and XLYC1802024), Liaoning Key Industrial Program (2019JH1/10100014), The Innovation Team of Northeastern University, and Global Talents Recruitment Program endowed by the Chinese government for their financial support. We thank the State Key Laboratory of Solidification Processing, Northwestern Polytechnical University (Grant No. SKLSP201805), Shagang Steel, and Lincoln Electric China. This work is also funded in part by the National Research Foundation of South Africa (BRICS171211293679).

APPENDIX A: ΔG CALCULATIONS FOR POSSIBLE DECARBURIZATION REACTIONS IN SUBMERGED ARC WELDING

The ΔG values of possible decarburization reactions were calculated by FactSage 6.4.^[33] The reaction module in FactSage was applied using FToxid, FSstel, and FactPS databases. The ΔG values for the reactions were adjusted to present dilute solute concentrations of C, Si, O, and Mn at one mass percent reference state in liquid Fe by using the free energy of solution values from the literature.^[34] The calculations were performed from 1773 (melting point of iron) to 2573 K (temperature of the hot spot at the arc root).^[24] The ΔG values were calculated with the following assumptions and summarized in Figure A1.

1. The setting of partial pressures of gases (O₂, SiO, and CO) was based on the fact that their partial pressures in the plasma are much smaller than unity.^[15]
2. The P_{O_2} value of 2.57×10^{-5} atm is the equilibrium P_{O_2} for the FeO-Fe system at 2573 K with unit activities of FeO and Fe.^[35]
3. The setting of maximum activities of SiO₂ and MnO expected in CaF₂-free flux (Flux F-12) was based on the assumption that the addition of CaF₂ to the flux has a dilution effect on MnO and may react with SiO₂ (via Reaction [A1]) to lower their activities in the slag.^[11,16] The activities of SiO₂ and MnO were referenced from the work of Rao and Gaskell,^[36] as it was reported that activity data of steelmaking could be used in SAW in terms of thermodynamic analysis.^[18,23,25]



4. The setting of FeO activity was based on the approximate FeO level analyzed in the post-weld slags in our previous studies, assuming the ideal

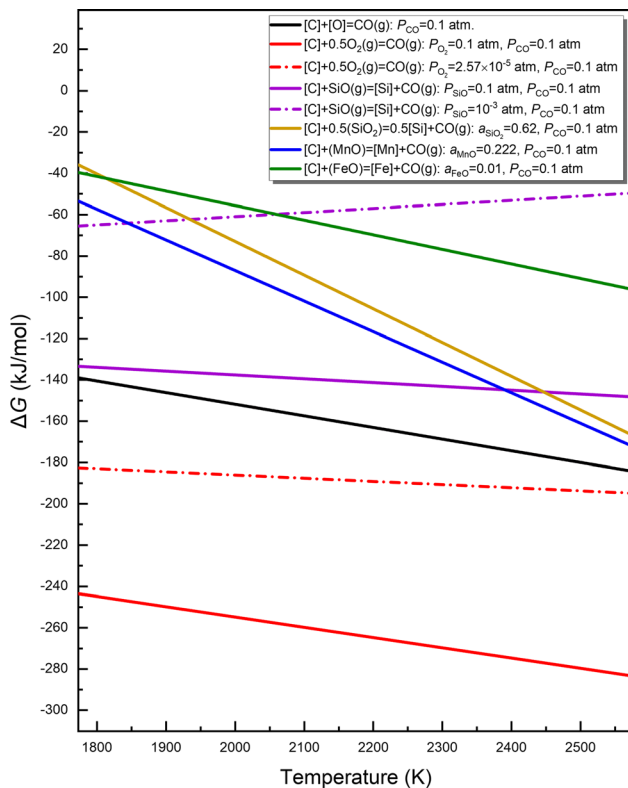


Fig. A1—Calculated ΔG values for possible decarburization reactions in SAW.

behavior of FeO in the slags at low FeO concentrations.^[16,17]

REFERENCES

- C. Chai: *Slag-Metal Reactions During Flux Shielded Arc Welding*, Massachusetts Institute of Technology, Cambridge, MA, 1980.
- D. Loder, S. Michelic, A. Mayerhofer, and C. Bernhard: *Metall. Mater. Trans. B*, 2017, vol. 48B, pp. 1992–2006.
- G. Evans: *Weld. J.*, 1983, vol. 19, pp. 133–320.
- R. Farrar and P. Harrison: *J. Mater. Sci.*, 1987, vol. 22, pp. 3812–20.
- S. Kou: *Welding Metallurgy*, 2nd ed., Wiley, New York, NY, 2003, pp. 22–95.
- V. Sengupta, D. Havrylov, and P. Mendez: *Weld. J.*, 2019, vol. 98, pp. 283–313.
- T. Lau, G. Weatherly, and A. McLean: *Weld. J.*, 1985, vol. 64, pp. 343–47.
- J. Indacochea, M. Blander, N. Christensen, and D. Olson: *Metall. Mater. Trans. B*, 1985, vol. 16B, pp. 237–45.
- U. Mitra and T. Eagar: *Metall. Mater. Trans. B*, 1991, vol. 22B, pp. 83–100.
- C. Natalie, D. Olson, and M. Blander: *Ann. Rev. Mater. Sci.*, 1986, vol. 16, pp. 389–413.
- C. Chai and T. Eagar: *Weld. J.*, 1982, vol. 61, pp. 229–32.
- T. Eagar: *Weld. J.*, 1978, vol. 57, pp. 76–80.
- K. Bang, C. Park, H. Jung, and J. Lee: *Met. Mater. Int.*, 2009, vol. 15, pp. 471–77.
- T. Lau, G. Weatherly, and A. McLean: *Weld. J.*, 1986, vol. 65, pp. 343–47.
- U. Mitra: *Kinetics of Slag Metal Reactions during Submerged Arc Welding of Steel*, Massachusetts Institute of Technology, Cambridge, MA, 1984.
- J. Zhang, T. Coetsee, and C. Wang: *Metall. Mater. Trans. B*, 2020, vol. 51B, pp. 16–21.
- J. Zhang, T. Coetsee, H. Dong, and C. Wang: *Metall. Mater. Trans. B*, 2020, <https://doi.org/10.1007/s11663-020-01821-z>.
- C. Chai and T. Eagar: *Metall. Mater. Trans. B*, 1981, vol. 12B, pp. 539–47.
- U. Mitra and T. Eagar: *Metall. Mater. Trans. A*, 1984, vol. 15A, pp. 217–27.
- U. Mitra and T. Eagar: *Metall. Mater. Trans. B*, 1991, vol. 22B, pp. 73–81.
- U. Mitra and T. Eagar: *Metall. Mater. Trans. B*, 1991, vol. 22B, pp. 65–71.
- J. Zhang, J. Leng, and C. Wang: *Metall. Mater. Trans. B*, 2019, vol. 50B, pp. 2083–87.
- C. Dallam, S. Liu, and D. Olson: *Weld. J.*, 1985, vol. 64, pp. 140–51.
- D. Olson, S. Liu, R.H. Frost, G. Edwards and D. Fleming: *Nature and Behavior of Fluxes Used for Welding*, ASM Handbook, Materials Park, OH, 1993, vol. 6, pp. 43–54.
- P. Burck, J. Indacochea, and D. Olson: *Weld. J.*, 1990, vol. 3, pp. 115–22.
- F. Richardson: *Proc. Int. Symp. on Chem. Metall. of Iron and Steel*, 1973, pp. 82–92.
- U.T. Gonzenbach, A.R. Studart, E. Tervoort, and L.J. Gauckler: *J. Am. Ceram. Soc.*, 2007, vol. 90, pp. 16–22.
- K.C. Mills: *Slag Atlas*, 2nd ed., Verlag Stahleisen GmbH, Düsseldorf, 1995.
- S. Hara and K. Ogino: *ISIJ Int.*, 1992, vol. 32, pp. 81–6.
- K. Mills and B. Keene: *Int. Met. Rev.*, 1981, vol. 26, pp. 21–69.
- S. Tulliani, T. Boniszewski, and N. Eaton: *Weld. Metal Fabric.*, 1969, vol. 37, pp. 327–39.
- J. Ito and M. Nakanishi: *Sumitomo Search*, 1976, pp. 42–62.
- C. Bale, P. Chartrand, S. Degterov, G. Eriksson, K. Hack, R. Mahfoud, J. Melançon, A. Pelton, and S. Petersen: *Calphad*, 2002, vol. 26, pp. 189–228.
- L. Coudurier, D. Hopkins, and I. Wilkomirsky: *Fundamentals of Metallurgical Processes*, 2nd ed., Pergamon Press, Oxford, 1985, pp. 265–74.
- K. Sasaki and Y. Mizukami: *ISIJ Int.*, 1996, vol. 36, pp. 388–94.
- B. Rao and D. Gaskell: *Metall. Mater. Trans. B*, 1981, vol. 12, pp. 311–17.

Publisher's Note Springer Nature remains neutral with regard to jurisdictional claims in published maps and institutional affiliations.